ACS Biomaterials SCIENCE & ENGINEERING

pubs.acs.org/journal/abseba

Article

Effects of a Gradated Fluid Shear Environment on Mesenchymal Stromal Cell Chondrogenic Fate

Terreill J. Robertson, II, Alec W. Schuler, Pakkanpat P. Pondipornnont, Ryan R. Driskell, Lawrence J. Bonassar, Arda Gozen, Wenji Dong, David B. Thiessen, and Bernard J. Van Wie*

Cite This: https://doi.org/10.1021/acsbiomaterials.5c01183

Read Online

ACCESS | Metrics & More | Article Recommendations | Supporting Information

ABSTRACT: Recreating articular cartilage trilayered patterning for an engineered in vitro cell construct holds promise for advancing cartilage's repair efforts. Our approach involves the development of a multichambered perfusion tissue bioreactor that regulates fluid shear stress levels similar to the gradated hydrodynamic environment in articular cartilage. COMSOL modeling reveals our tapered cell chamber design will produce three different shear levels, high in the 22−41 mPa range, medium in the 4.5−8.4 mPa range, and low in the 2.2−3.8 mPa range and distributed across the surface of our mesenchymal stromal cell (MSC) encapsulated construct. In a 14 day bioreactor culture, we assess how the fluid shear magnitude and cell vertical location within a 3D construct influence cell chondrogenesis. Notably, Sox9 expression for MSCs cultivated in our reactor shows spatially patterned gene upregulations that encode key chondrogenic marker proteins. Beginning with the high shear stress region, lubricin and type II collagen gene increases of 410 and 370-fold indicate cell movement toward a superficial zone architype, which is further supported by histological and immunohistochemical stains illustrating the formation of a dense proteoglycan matrix enriched with lubricin, versican, and collagen types I and II molecules. For the medium shear stress region, high aggrecan and type II collagen gene expressions of 2.3 and 400-fold, respectively, along with high proteoglycan analyses, show movement toward a superficial/midzone cartilage archetype. For low shear stress regions, higher collagen type II and X gene upregulations of 550- and 8300-fold, the latter being 2× of that for the high shear regime, indicate cell movement with deep zone characteristics. Collectively, biochemical analysis, histology, and gene expression data demonstrated that our fluid shear bioreactor induced a stratified structure within tissue-engineered constructs, demonstrating the feasibility of using this approach to recapitulate the structure of native articular cartilage.

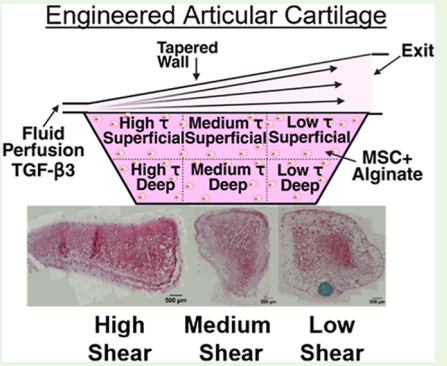

KEYWORDS: *biomanufacturing, perfusion bioreactor, cell differentiation, cartilage, mesenchymal stromal cells*

INTRODUCTION

Manufacturing an organized extracellular matrix (ECM) that is representative of striated articular cartilage (AC) regions is crucial for restoring the native mechanical functionality that is disrupted in osteoarthritis (OA). Promising cartilage tissue engineering methods such as matrix-induced autologous chondrocyte implantation (MACI) seek to slow OA progression; however, potential drawbacks of this strategy include chondrocyte dedifferentiation, reduced tissue mechanics, and improper tissue integration.[1,2] A more fundamental approach involves understanding how a gradated fluid shear stress environment affects the trajectory of cell differentiation toward a heterogeneous chondrogenic cell population that parallels what is observed in native AC. In native tissue conditions, high levels of synovial fluid shear stresses near the superficial region contribute to the "elongated" morphology of AChs,[3] corresponding to the secretion of lubricin and collagen type II (COL2A1).[4,5] Beneath the top layer, the magnitude of fluid shear stress is lessened, and ACh morphology becomes rounded, which promotes predominant COL2A1 and aggrecan (ACAN) expression. For deep zone AC where fluid shear is minimal, cells orient themselves in a columnar organization and begin to produce a mineralized matrix marked by type X collagen (COL10A1) protein.[6] This understanding of the cell microenvironment has motivated researchers to replicate these important features within a bioreactor to support chondrocyte proliferation and differentiation.[7−9]

Progress in mimicking AC physiology has been achieved through bioreactor development, which ensures proper biological cues for tissue production. Perfusion-based bioreactor systems are exceptional candidates for investigating chondrogenesis because they provide a constant distribution of nutrients required for cell survival in addition to supplying fluid

Received: July 2, 2025
Revised: September 18, 2025
Accepted: September 22, 2025

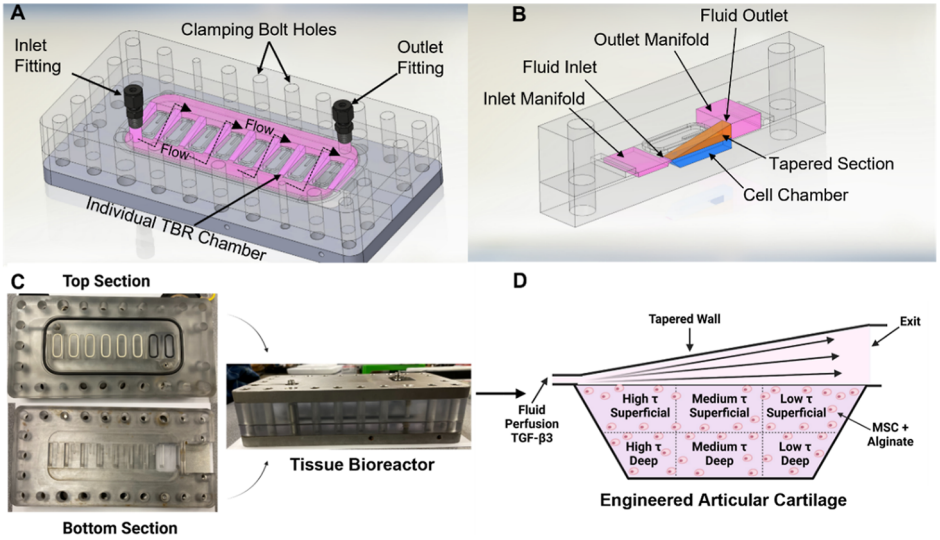

Figure 1. TBR chamber design. (A) CAD drawing illustrates a multichambered TBR design in which fluid first fills an inlet manifold and then distributes to individual chambers. (B) Tapered wall geometry creates gradated fluid velocity across the top surface of cross-linked cell-laden alginate constructs retained in the bioreactor chamber. (C) Constructed TBR with multiple chambers with O-ring seals with a schematic. (D) Our strategy for assessing cell differentiation with respect to the changing hydrodynamic environment across the construct surface as well as construct depth.

shear levels representative of native AC biomechanics.[10−12] Fluid shear mechanical loading of cells within such bioreactors has led to improvements in glycosaminoglycan (GAG) and collagen content upward of 184% and 155%, respectively, yielding an enhanced tensile modulus.[13−16] Additional studies show fluid shear stress affects COL2A1 expression compared to static cultures.[17,18] These findings indicate that direct fluid perfusion promotes chondrogenic activity; however, there is limited work correlating surface shear magnitudes to cellular differentiation in addition to chondrogenic commitment as a function of cell location within a construct. Moreover, native AC is a trilayered tissue with distinct gradients in ECM proteins and stiffness properties in addition to different cell morphologies and, more importantly, functional role.[1,2,19,20] Developing a cell construct with a similar regional variation in chondrogenic properties is expected to be aided by the creation of a gradated hydrodynamic environment that regulates cell differentiation.

Our approach involves cultivating alginate-encapsulated mesenchymal stromal cells (MSCs) in a multichambered, tapered perfusion bioreactor. This system maintains a broad range of surface fluid shear stresses to create an environment serving to commit MSCs to a heterogeneous chondrogenic fate. This method provides a unique approach for investigating how different cell regions encapsulated within a single alginate construct respond to a wide range of surface fluid shears. We present and assess the movement of MSCs along lineages marked by expression of chondrogenic mRNAs and the manufacture of characteristic AC proteins for striated ECM synthesis.

METHODS

Bioreactor Design and Assembly. Our perfusion bioreactor is designed to provide a longitudinal gradient in shear stress across the surfaces of 9 individual scaffold constructs, each in their own well, functioning in parallel. The reactor consists of two sections: the lower half with wells containing cell-aden scaffolds and the upper half, which contains tapered flow sections as shown in Figure 1A through C. Wells measure 20 mm long by 5 mm wide and are 4 mm deep to mimic the thickness of articular cartilage. The upper section has a rectangular inlet 0.7 mm in height and an exit 6.7 mm in height for an overall taper angle of 11.4°, which yields variable shear stresses that are highest at the inlet and lowest at the outlet. All wells are provided fluid medium via the inlet manifold, which travels across the construct surface and then exits into the outlet manifold. There are 3/16 in. tube fittings at the entrance and exit of corresponding manifolds for flow in an overall Z-pattern as shown in Figure 1A. Both sections of the reactor are machined from polycarbonate and are joined together with a fluoroelastomer O-ring between them, clamped by two 1/2″ 304 stainless steel plates secured with 21 bolts. Smaller individual O-rings circle the blank spaces between the individual wells to prevent fluid leakage between the two halves and separate wells from one another.

COMSOL Fluid Dynamics Simulation. Computational fluid dynamics modeling was performed using COMSOL Multiphysics to assess fluid flow distribution and quantify fluid flow properties for our multichambered perfusion bioreactor. A laminar flow simulation was selected for our 3D model where an overall feed flow rate of 20 mL/min was chosen for the bioreactor inlet with the assumption of incompressible flow and no wall slip at the liquid/construct interface. A "physics-controlled" mesh with "very fine" spacing was selected for the simulation. Flow parameters for the reactor were solved using the steady-state form of the Navier−Stoke's equation shown in eq 1

$$\rho(\boldsymbol{u}\cdot\nabla)\boldsymbol{u} = \nabla\cdot[-p\tilde{I} + \tilde{\tau}] \quad (1)$$

where the viscous stress tensor shown in eq 2 is

$$\tilde{\tau} = \mu[\nabla\boldsymbol{u} + (\nabla\boldsymbol{u})^T] \quad (2)$$

Fluid density (ρ) and viscosity (μ) are taken as those of water. Fluid shear stresses created at the interface between the liquid and the construct were determined from the dot product of the surface normal and the viscous stress tensor.

Data obtained from the simulation provided insight into the system delivery of similar fluid flow rates for each cell chamber and allowed us to validate our strategy for developing an improved hydrodynamic environment for AC production.

Cell Culture. All cell culture products were supplied by Gibco, with the exceptions indicated for different vendors. While current best practices are to use pooled MSCs from three or more donors,[21] for this initial baseline study we selected primary human MSCs from a 20 year old female donor purchased from RoosterBio, Inc. We note that

https://doi.org/10.1021/acsbiomaterials.5c01183
ACS Biomater. Sci. Eng. XXXX, XXX, XXX−XXX

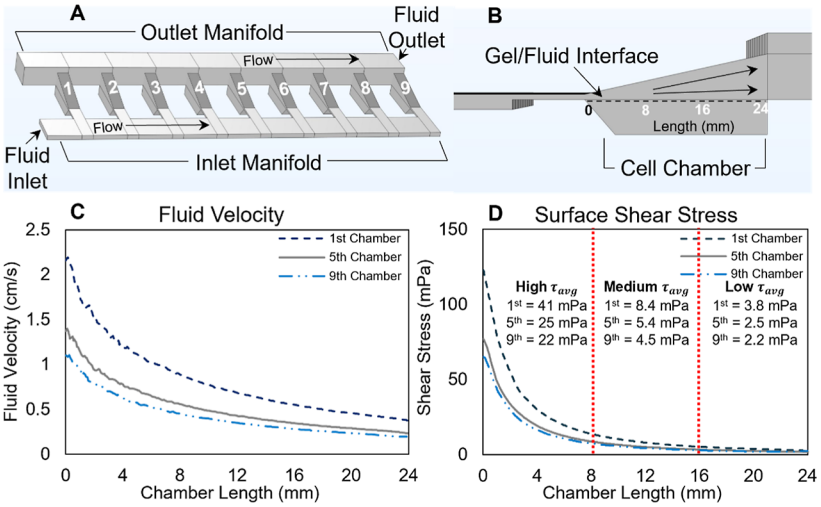

Figure 2. COMSOL Multiphysics modeling. (A) 3D COMSOL geometry of the perfusion bioreactor assembly along with a side-view illustration. (B) Further detail for respective perfused fluid and cell chamber domains. (C) Modeled laminar flow simulation for chambers 1, 5, and 9 reveals an exponential drop in fluid velocity for each chamber. (D) Surface shear stresses showing an exponential drop. Shear averages for chambers 1, 5, and 9 are listed, and there is significant overlap for all chambers in each of the 3 ranges of high, medium, and low fluid shear regimes.

MSCs from younger females have been shown to be more proliferative[22] and therefore easier to expand to larger numbers, though they are less chondrogenic than those from males.[23] Hence, should results prove favorable here, we might expect in future studies to see even better results when using male-derived MSCs or pooled MSCs. MSCs were grown in T-175 cell culture flasks containing α-MEM medium consisting of 10% fetal bovine serum (FBS) (Cytivia), 1% penicillin/streptomycin, and 1% L-glutamine. Once 90% confluence was reached, cells were washed with phosphate buffered saline (PBS), released from the surface using trypsin−EDTA, then passaged up to six generations, and finally cryopreserved at −80 °C until usage.

Cell-Laden Scaffold. Cell-laden constructs were created by encapsulating MSCs in 1.5% (w/v) ultrapure alginate acquired from Novamatrix.[24,25] This was achieved by resuspending 1×10^7 cells/mL[26,27] in sterile-filtered alginate solution, pipetting 400 μL of the solution into individual TBR chambers (9 chambers total), and finally cross-linking constructs by overlaying the gels with 102 mM calcium chloride[28] solution for 50 min to ensure scaffold gelation. Similarly, static hydrogel controls were generated using the same process but with a separate mold containing a similar geometry (3 chambers total). Constructs were washed with a PBS solution after gelation.

Chondrogenic differentiation of MSC encapsulated constructs was induced using a culture medium cocktail[29] composed of DMEM/F-12, containing 10% FBS, 2 mM L-glutamine, 100 U/mL pen/strep, 2.5 μg/mL fungizone, 10 ng/mL TGF-β3 (PeproTech), 100 nM dexamethasone, and 50 μg/mL ascorbic acid. For both the static control and perfused experimental constructs, the culture medium was replaced every 3 days over a 14 day period. For the control group, 3 gels were used with individual scaffolds placed in a 6-well plate. Culture medium for the experimental group was perfused at 20 mL/min through our perfusion bioreactor using a peristaltic pump, which resulted in flow being divided among the 9 individual chambers. Two separate sets of experiments were performed under the same conditions in which biochemical content, mRNA expression, and data on cell viability using the validated Invitrogen Live/Dead assay were collected for one study, while histology and immunofluorescence staining were performed for the other. Cell viability methodology, and the results are presented in Figure S2 of the Supporting Information.

Biochemical Content. Cell-laden constructs were tested for total glycosaminoglycan (GAG) and collagen to assess the ECM synthesis and subsequent secretion. For GAG and DNA quantification, the construct was thinly sliced into $8 \times 2.5 \times 2$ mm ($L \times W \times H$) side-by-side sections from three separate bioreactor wells (i.e., $n = 3$), resulting in duplicate side-by-side samples for the surface and deep zones of the constructs for all three shear regimes, high, medium, and low. These were digested for 16 h overnight in 125 μg/mL papain dissolved in pH 6.5 sodium phosphate buffer containing 10 mM L-cysteine and 10 mM EDTA at 60 °C. Samples for collagen quantification were digested for 16 h in a 0.1 mg/mL pepsin dissolved in 0.5 M acetic acid at 4 °C. For respective colorimetric quantitation of sulfated proteoglycans (GAGs) and collagen, measurements were completed using one section side for Blyscan and the adjacent side for Sircol assay kits, both supplied by Biocolor, Ltd. Biochemical content was normalized to DNA quantified by papain extracts using the Quant-iT PicoGreen dsDNA Assay kit (Invitrogen).

mRNA Expression. Quantitative Real Time Polymerase Chain Reaction (qRT-PCR) was used to measure chondrogenic and nonchondrogenic mRNA expression in MSCs. Sectioned slices of cell-laden samples taken from three separate parallel chambers ($8 \times 5 \times 2$ mm; $L \times W \times H$) were washed with PBS solution prior to cell isolation by immersing the constructs in 55 mM citrate buffer. Total RNA was isolated using a Purelink mini-RNA kit (Invitrogen), and its quantity was measured using a nanodrop spectrophotometer. Superscript IV Vilo (Invitrogen) was used to reverse transcribe RNA to cDNA for quantitative mRNA expression of Sox9, aggrecan (ACAN), lubricin, collagen types I, II, and X, and RUNX2. GAPDH served as an endogenous control, and experimental samples were normalized to day 0 cells to compare relative fold changes across groups. Primer information corresponding to genes of interest can be found in Table S1 in Supporting Information.

Histology. After culture, cell constructs were first washed with Dulbecco's phosphate-buffered saline solution and then immersed in 4% paraformaldehyde solution for 30 min at room temperature. Fixation of tissue constructs was then followed by a series of 3 DPBS immersions, 20 min each. Samples were stored in 70% ethanol prior to tissue paraffinization. In this process, the samples were dehydrated by placing them in an automatic sample preparation instrument (TP1020, Leica) and then immersing them sequentially in each of the following solutions for 30 min per immersion: xylene, then 70% ethanol, followed by immersions in 75%, 95%, and 100% ethanol. This sequence was replicated 2 times. Fixed hydrogels were finally embedded in paraffin wax, then sectioned into 7 μm slices using a microtome, and baked overnight at 40 °C onto positively charged Leica slides. Sample orientation is provided in Figure S1 in Supporting Information. Sectioned tissue samples were stained for ECM structure, sulfated GAG synthesis, and proteoglycan production using the respective Hematoxylin and Eosin (H&E), 1% Alcian Blue, and 1% Safranin O histological stains. Stained samples were visualized

https://doi.org/10.1021/acsbiomaterials.5c01183
ACS Biomater. Sci. Eng. XXXX, XXX, XXX−XXX

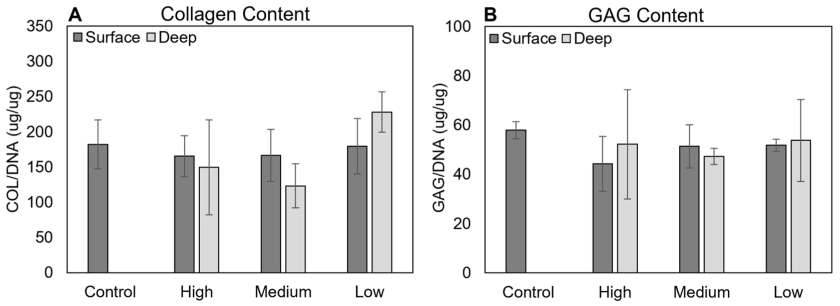

Figure 3. Biochemical content indicating normalized total collagen (A) and GAG secretions (B) for cell cultures in nonperfused conditions vs those in gradated perfused conditions. (N = 3).

and photographed under a 20× objective using a Nikon light microscope.

Immunohistochemical (IHC) Staining. Slides containing tissue samples were deparaffinized to dewax the slides by immersing them within plastic Coplin jars for two 5 min rinses in xylene (Sigma-Aldrich) and then in a series of 3 min rinses, twice each, with 100%, 95%, and 70% ethanol and finally dH_2O. Following these rinses, the slides were incubated one time in a solution containing 5 mM $CaCl_2$ (J.T. Baker) and 100 mM Tris−HCl (RPI) pH 7.3 for 1 h at 37 °C. Then the slides were incubated in 0.1% hyaluronidase (Sigma-Aldrich) and PBS for 20 min at 37 °C to increase the pore size and reveal proteins of interest. Following this, the slides were incubated in 10× PBS containing 5% bovine serum (Fisher BioReagents) and 0.3% Triton X-100 (Thermo Scientific) in a humidity incubation box for 1 h at room temperature. The slides were incubated with primary antibodies (specific details located in Supporting Information) diluted in 10× containing 1% bovine serum (Fisher BioReagents) and 0.3% Triton X-100 (Thermo Scientific) overnight at 4 °C. The next day, the slides were incubated with secondary antibodies in 10× PBS containing 5% bovine serum and 0.3% Triton X-100 for 2 h at 4 °C. Then, the slides were rinsed 2 times with 1× PBS for 5 min each time. Table S2 in the Supporting Information shows the protein markers of interest, primary and secondary antibodies used, and fluorescence color. Care was taken to divide slide staining protocols into groups with differing primary antibody hosts. Immunofluorescence-stained tissue slides were visualized under confocal microscopy at 20× magnification to identify specific protein deposition and cell markers.

Statistics. Statistical analyses were completed using GraphPad Software, where a two-way analysis of variance (ANOVA) followed by a posthoc Tukey's test provided statistical insight for assessing cell expression parameters as a function of fluid shear magnitude and cell location within alginate constructs.

RESULTS

Bioreactor Modeling. First, we assess the change in fluid pressure distribution across the inlet manifold as well as through individual cell chambers, outlined in Figure 2A, to determine that fluid flows for successive chambers 1, 5, and 9 will be fairly equal. COMSOL modeling results show that pressures in the inlet manifold will begin at 4.8 Pa at the entrance of chamber 1 and then decrease by 2.2 Pa to reach a pressure of 2.6 Pa at the entrance of the ninth chamber. Flows through each chamber are driven by corresponding pressure drops of 3.5, 2.5, and 2.4 Pa for respective chambers 1, 5, and 9. We realize from Figure 2B that the velocity will decrease across the length of the tapered chamber due to increasing cross-sectional area. Figure 2C supports this, where fluid flows exhibit higher velocities of 2.4, 1.4, and 1.1 cm/s at the beginning of reactor chambers 1, 5, and 9, tapering exponentially downward across the chamber length to corresponding magnitudes of 0.4, 0.2, and 0.2 cm/s at the exits. Flow distribution was validated through injection of dye, with selected videography frames shown in the Supporting Information along with a corresponding link to the video, where the flow rate of dye across the inlet manifold is reduced and the speed at which dye proceeds from inlet to outlet is reduced slightly from one successive chamber to another.

Our tapered perfusion bioreactor with varying fluid velocity across each cell chamber leads to changing viscous force distribution across cell-laden constructs. Our simulation supports this premise, where we see an exponential decay of fluid shear stresses, provided in Figure 2D, across the length of our cell chamber. We designate hydrodynamic shears as either high, medium, or low, separated into 8 mm segments, which correspond to average shear magnitudes of 41, 8.4, and 3.8 mPa for chamber 1. When comparing these findings to chambers 5 and 9, average viscous shears are respectively calculated as 25 and 22 mPa for high, 5.4 and 4.5 mPa for medium, and 2.5 and 2.2 mPa for low fluid shears. We note there is significant overlap for average fluid shear regimes between parallel chambers when transitioning from a 22 to 41 mPa range for high, 4.5 to 8.4 mPa for medium, and finally 2.2 to 3.8 mPa for low shear ranges. Based on our modeling predictions and flow distribution confirmation through dye injections (Supporting Information document), we are confident that our multichambered perfusion bioreactor maintains similar hydrodynamic environment sets, high, medium, and low, for all the individual cell chambers. Biochemical content, mRNA expression, and histological/IHC staining findings from our 14 day bioreactor culture will further demonstrate that our gradated hydrodynamic environment induces chondrogenesis, which differs region-by-region for surface shears as well as with tissue depth.

Biochemical Content. Analysis of total collagen and total GAG as a function of surface shear and depth compared to static control offers an initial assessment of tissue synthesis and whether we might expect variations in the subtypes of matrix components manufactured by the cells. First, we note from Figure 3A,B for total collagen/DNA and GAG/DNA there are no statistically significant differences between the static control and any portions of the tissue construct exposed to varying levels of shear on the surface, whether for the upper surface or deeper regions. This indicates all tissues contain viable healthy cells producing the anticipated types of proteins typically present in ECM. There are small differences, such as total collagen localization near the construct surface for high and medium surface shears and deeper in the construct for low surface shears. In addition, small GAG increases exist for medium- to low-surface-shear cell regions. These small but apparent differences offer some indication that while the overall totals in the more abundant and common ECM

https://doi.org/10.1021/acsbiomaterials.5c01183
ACS Biomater. Sci. Eng. XXXX, XXX, XXX−XXX

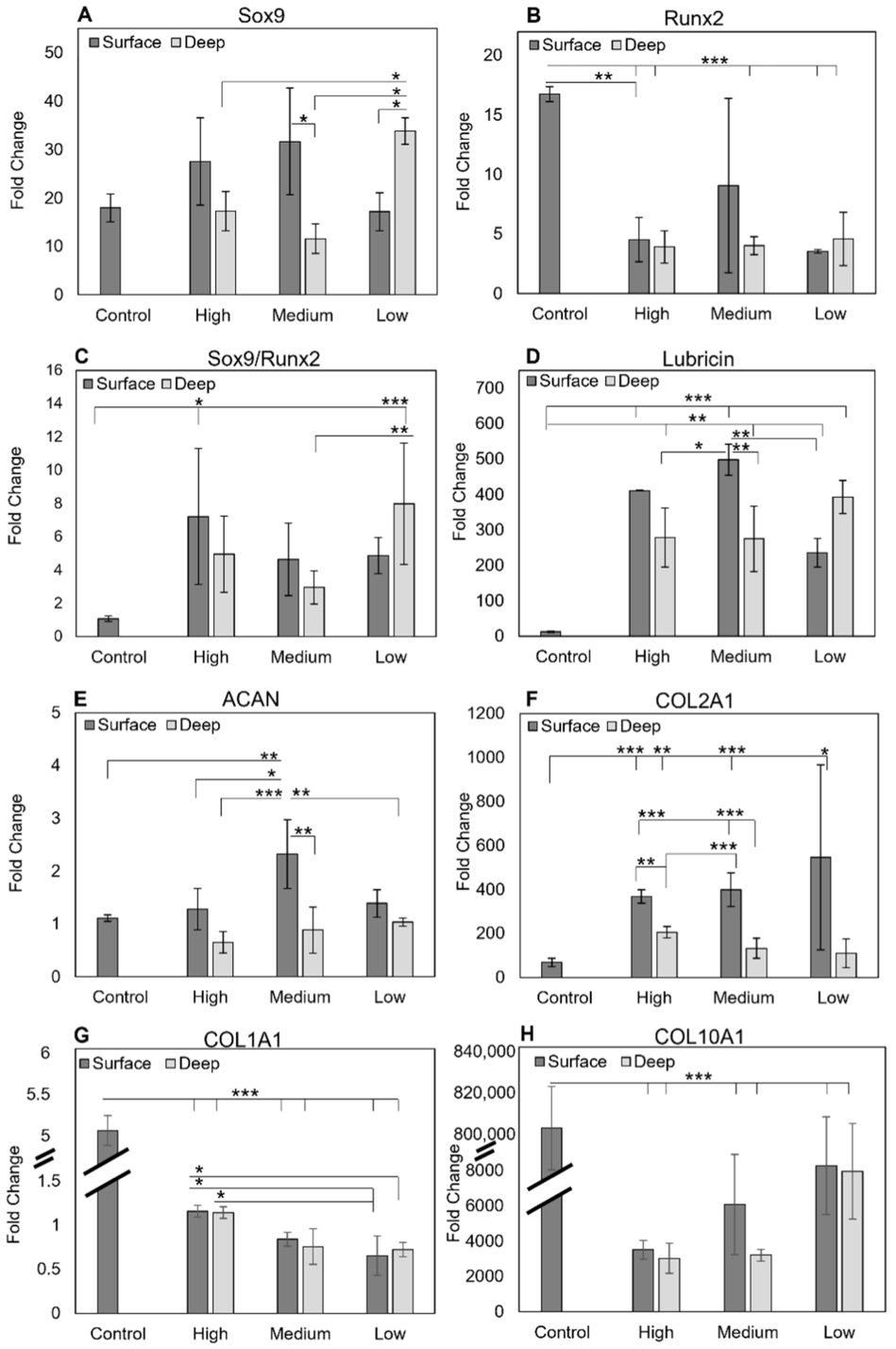

Figure 4. mRNA for Sox9 (A), Runx2 (B), Sox9/Runx2 (C), lubricin (D), ACAN (E), COL2A1 (F), COL1A1 (G), and COL10A1 (H) relative to day 0 MSCs. Results are shown for cells exposed to nonperfused vs perfused cultures at high, medium, and low surface shears and surface vs deep experimental conditions. (N = 3, *, **, ***: p < 0.05, <0.01, <0.001).

constituents remain relatively constant, much more may be happening in terms of the subtypes of proteins produced and that precise control of such stimuli is critically important for the future of tissue engineering in the biomanufacture of tissues with anisotropic properties.

mRNA Expression. Investigating a wide assortment of expressed genes for experimental samples enables us to determine how a gradated hydrodynamic environment affects gene up- or down-regulation toward chondrogenic or, alternatively, more hypertrophic cell differentiation. Beginning with chondrogenic transcription factor Sox9,[30] findings displayed in Figure 4A indicate gene upregulation for cells grown in a perfused environment where distinct regions in our engineered construct show strong gene expression. This observation is supported by increased Sox9 expression, compared to static controls, in the 1.5−1.9-fold range for MSCs stimulated by high to medium surface shears and those deep within the tissue with surfaces stimulated by low fluid shears. Simultaneously, our bioreactor significantly reduces osteogenic Runx2 transcription factor marked by a fold change

https://doi.org/10.1021/acsbiomaterials.5c01183
ACS Biomater. Sci. Eng. XXXX, XXX, XXX−XXX

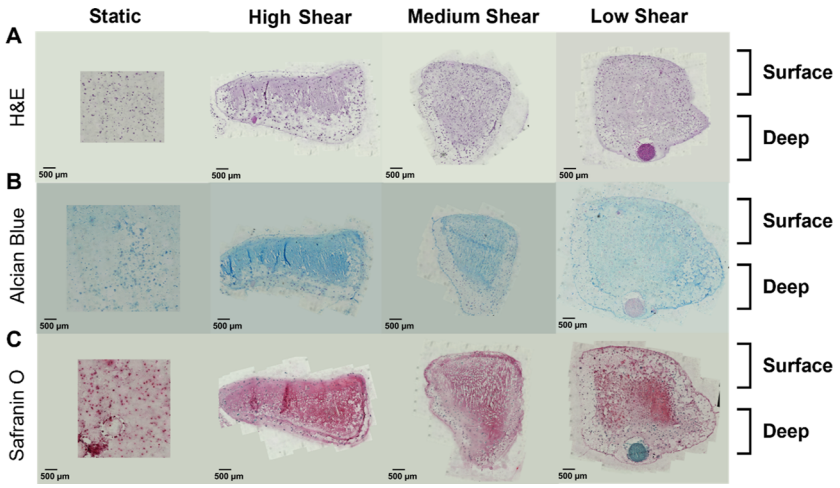

Figure 5. Histological staining of cell-laden scaffolds shows definitive chondrogenesis with respect to static controls and more dense staining at higher shear stresses. (A) H&E staining showing ECM structure, (B) Alcian Blue staining for sulfated GAG, and (C) Safranin O staining for proteoglycan. 20× magnification.

in the 0.21−0.45 range (p = 0.0005−0.055) as indicated in Figure 4B. Sox9/Runx2 ratios in Figure 4C accentuate our argument that gradated fluid perfusion serves to commit MSCs toward a chondrogenic lineage where these ratios are significantly upregulated in all cases and by as much as 6.7-fold for cells stimulated by high fluid surface shears (p = 0.02) and 7.4-fold for cells beneath the tissue surface that are stimulated by low fluid surface shears (p = 0.001).

We monitored the expression of chondrogenic marker genes, including lubricin, ACAN, and collagen type II (COL2A1), and compared these mRNA profiles to those of fibrocartilage collagen types I (COL1A1) and hypertrophic type X (COL10A1). Figure 4D−F demonstrates that our hydrodynamic environment improves cell chondrogenic expression, supported by upregulated fold-change ranges of 20−40 for lubricin (p = 0.0001−0.009), 1.2−2.1 for ACAN (p = 0.008−0.096), and 2−8-fold for COL2A1 (p = 0.0001−0.03). When comparing these results to control samples that exhibit hypertrophic expression, we see further evidence of chondrogenic behavior in Figure 4G,H, where the expression of COL1A1 and COL10A1 is dramatically reduced in a perfused cell culture environment. Downregulated COL1A1 and COL10A1 correspond to fold changes in the 0.13−0.22 (p < 0.0001) and 0.001−0.004 ranges (p < 0.0001) compared to static controls. Hence, the trends in mRNA data for lubricin, COL2A1, COL1A1, and COL10A1 data agree with what we would expect with the Sox9/Runx2 regulatory gene ratios.

In our analysis of biochemical content outlined in Figure 3, there was some indication that different surface fluid shear magnitudes influence cell ability to secrete total amounts of protein within certain categories, i.e., collagens and glycosaminoglycans. We expected that tracking gene expression profiles would further reveal specific mRNA types that are upregulated in our engineered tissue grown in a gradated fluid shear environment. Indeed, our reporting of expressed genes agrees with this premise, where maximal upregulation of COL1A1 shows a significant 1.8-fold increase for cells stimulated by high surface fluid shears compared to low surface fluid shears (p = 0.01). A similar trend is also observed for MSCs exposed to medium surface fluid shears, where lubricin is maximally expressed and significantly higher by 1.2 and 2.1-fold than that in both corresponding high and low surface fluid shears, while ACAN is higher by 1.8−1.7-fold than high and low surface fluid shears (p = 0.054 and 0.002). While not statistically significant, we also see that certain genes in our engineered tissue are more prominently expressed in distinct tissue regions stimulated by the various viscous shear levels. This effect is evident for MSCs stimulated by high to medium surface fluid shears, in which their expression of Sox9 is 1.6 and 1.8-fold higher than cells grown under low surface fluid shears, respectively. We also see this for cells exposed to the low surface fluid hydrodynamic environment, where expression is increased to the 1.4−1.5-fold range for COL2A1 and the 1.4−2.4-fold range for COL10A1 over that for the high and medium shear ranges. In summary, our controlled delivery of gradated fluid shears across the top surface of alginate-encapsulated MSCs strongly influences gene expression profiles, thus creating a diverse gene-expressing cell population all within the same construct. More importantly, comparing these differences to how cells behave deep within the alginate matrix provides meaningful insight into how cells sense mechanical stimulation.

Our data show that mRNA profiles for Sox9, lubricin, ACAN, COL2A1, and COL1A1 illustrate significant localization near the cell construct surface, which differs from cells nearer the bottom. Respective Sox9 expression is 1.6-fold (p = 0.41) and 2.7-fold (p = 0.01) higher at the surface for cell regions stimulated by high and medium fluid shears than cell populations directly beneath them. In contrast, for low surface shear, we observe an opposite trend where Sox9 and lubricin for cells deeper beneath the surface exhibit higher expressions than those near the surface by respective 2.0-fold and 1.7-fold (p = 0.044 and 0.10) higher values. Correspondingly, we see localized expressions of lubricin, COL2A1, and ACAN for cells nearer the construct surface in comparison to those deeper in the tissues; for lubricin, localizations are 1.5 and 1.8-fold (p = 0.23 and 0.01) higher for respective high and medium shears; this is also supported by COL2A1 upregulations in the 1.8−5.0-fold range (p = 0.0001−0.05), and ACAN increases in the 1.3−2.6-fold range (p = 0.0015−0.89) for high, medium, and low shear cell regions. For COL1A1 there is an insignificant difference between expressions observed for cells relative to distance from the surface, but we do see for high shears that expression is on average 1.4 and 1.7-fold higher for the

https://doi.org/10.1021/acsbiomaterials.5c01183
ACS Biomater. Sci. Eng. XXXX, XXX, XXX−XXX

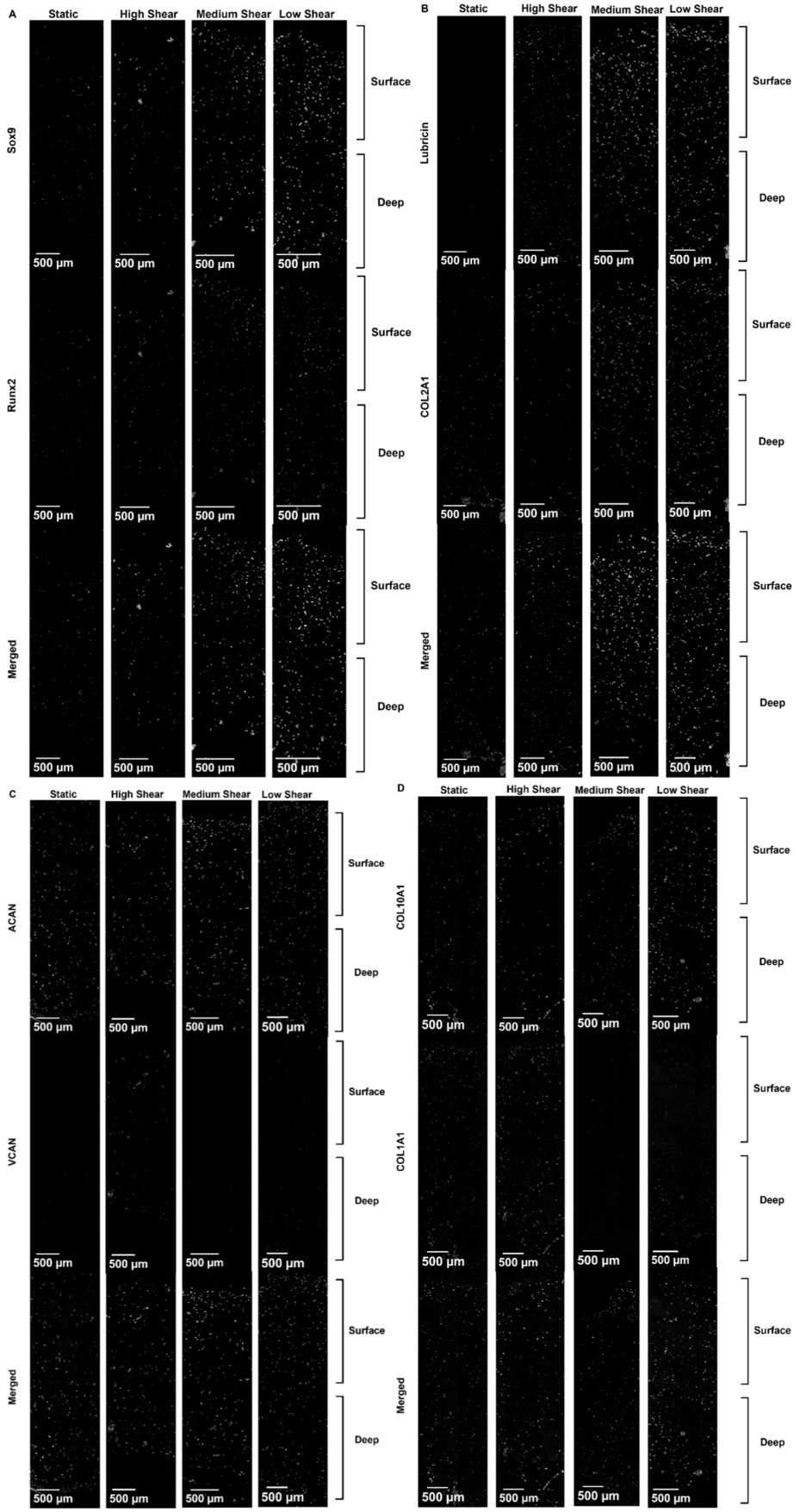

Figure 6. Region-by-region IHC protein staining for (A) Sox9/Runx2, (B) Lubricin/Type II collagen, (C) Aggrecan/Versican, and (D) collagen types I/X all captured at 20× magnification.

https://doi.org/10.1021/acsbiomaterials.5c01183
ACS Biomater. Sci. Eng. XXXX, XXX, XXX−XXX

Table 1. Findings for Regionally Directing Cell Chondrogenesis.[a,d]

Shear (τ) Surface / Deep	Key Cell Culture Findings	Conclusions	Literature
Static Control	**mRNA** ▲Runx2: 4.7-fold*** ▲Col10: 280-fold*** **Histology** Low sGAG & proteoglycan **IHC**: ▼Sox9; ▼Col2	• Significant expression of Runx2, Col1 and Col10 hypertrophic markers in addition to inferior matrix synthesis.	**mRNA**[31,32] ▼Sox9;▲Col10; ▲Col1 **ECM** [13,14] ▼ Col; ▼GAG **Protein**[7,15,16,31] ▼ACAN; ▼Lub
High τ 22 – 41 mPa **Surface**	**mRNA** ▲Lub: 33-fold*** ▲Col2: 5.4-fold*** ▼Col1: 0.22-fold*** **Histology** Surface localized proteins **IHC**: ▲VCAN; ▲Col	**Superficial Zone:** • Presence of Lub, Col2, and VCAN markers with noticeable Col1 levels (1.8-fold > Low τ surface) • High shear stresses yield cell characteristics supporting synovial joint formation	**100 mPa τ** [33] ▲ shear modulus 5 MPa **120 mPa τ** [7] ▲Lub; ▲ Col2 **50-210 mPa τ** [18] ▲ 66% shear modulus ▲ Safranin O staining for proteoglycans
High τ **Deep**	**mRNA** ▼Sox9: 0.96-fold ▼ACAN: 0.59-fold **Histology** Lower synthesized proteins **IHC**: ▲Sox9; ▼Col10	• Evidence of cell chondrogenesis but at a lower degree (0.67-fold Lub & 0.55-fold Col2 < High τ surface)	
Med. τ 4.5 – 8.4 mPa **Surface**	**mRNA** ▲Sox9: 1.8-fold*** ▲Lub: 40-fold*** ▲ACAN: 2.1-fold** **Histology** Surface localized proteins **IHC**: ▲Lub; ▲ ACAN	**Superficial/Middle Zone:** • Tissue region with strong chondrogenic commitment supported by expression of Sox9, Lub, and ACAN markers. • Cell characterizations for medium fluid shears show resemblance to Superficial/Middle zone AC.	**6.7 mPa τ** [34] ▲Col2 ▲Col1 WB[§] protein density **4.6 mPa τ** [8] ▲ maximal GAG production compared to higher fluid shears up to 56 mPa
Med τ **Deep**	**mRNA** ▼Sox9: 0.64-fold ▼ACAN: 0.8-fold **Histology** Less dense protein levels **IHC**: ▲Sox9; ▼Col1	• Similar observation as High τ deep (0.4-fold Sox9 & ACAN < Medium τ surface)	
Low τ 2.2 – 3.8 mPa **Surface**	**mRNA** ▼Sox9: 0.96-fold ▲Col2: 8.0-fold* ▼Col10: 0.01-fold*** **Histology** Less dense surface proteins **IHC**: ▲Col2; ▲Col10	**Deep[#] Zone:** • Dramatic shift in cell behavior with definitively higher Col2 & Col10 expression (1.5 & 2-fold > high τ) • Collagenous matrix formation at from low shear stresses resembles Deep zone AC.	**1.2 mPa τ** [34] ▲Col2/Col1 WB protein density **1 μm/sec** [13] ▲155% total collagen
Low τ **Deep**	**mRNA** ▲Sox9: 1.9-fold ▲Lub: 32-fold*** **Histology** Dense proteins deep within construct **IHC**: ▲Sox9; ▲Col10	• Sox9 & Lub gene expression levels contrast findings for other deep cell regions (2-fold Sox9 & 1.7-fold Lub)	**10 μm/sec** [31] ▲ 20-fold Sox9 & 108-fold COL2 mRNA upregulation

[a]Findings compared to static control samples; control values compared to averages for all shear samples; *$p < 0.05$, **$p < 0.01$, ***$p < 0.001$. [b]WB = western blot. [c]Refers to deep zone AC characteristics, which differ from our deep or subsurface cell region. [d]Key: increase (▲, green) or decrease (▼, green) in factors supporting chondrogenic differentiation; increase (▲, red) or decrease (▼, red) in factors representing less chondrogenic differentiation.

respective average medium and low shear values. For COL10A1, exposure to low surface shear indicates an apparent increase by an average of 2.5 and 1.9-fold compared to average values for the high and medium shears. Collectively, our data provide evidence that our tapered perfusion bioreactor differentiates cells toward a heterogeneous chondrogenic lineage where their gene expression is a resultant of a changing fluid environment and vertical depth throughout an alginate scaffold.

Histology. Further support of region-by-region chondrogenic variation is offered by histological staining. H&E, Alcian Blue, and Safranin O stains depicted in Figure 5A–C corroborate our gene expression findings where we see synthesis of a densely organized matrix contrasted to sparse tissue formation exhibited by static nonperfused samples. Primarily, these images reveal evidence of MSC chondrogenesis, in which sulfated GAG (sGAG) and proteoglycan protein markers, representative of cartilage formation, appear

https://doi.org/10.1021/acsbiomaterials.5c01183
ACS Biomater. Sci. Eng. XXXX, XXX, XXX−XXX

for stimulated samples. Comparisons that assess the effect of fluid shear distributions on chondrogenic tissue synthesis provide further evidence of anisotropic tissue production. Safranin O and Alcian Blue staining indicate region-by-region differences in tissue composition, showing patterned protein localization. In Figure 5B fluid shear stress magnitude affects sGAG accumulations, where dense Alcian blue stains for cell-encapsulated constructs exposed to high and medium surface fluid shears are contrasted by a less dense sGAG presence for construct regions stimulated by low surface fluid shear. This is also valid for AC proteoglycan content, where Safranin O stains depicted in Figure 5C indicate a similar observation in which we see concentrated staining at the surface of cell constructs grown under a high and medium hydrodynamic environment. Furthermore, this observation of surface-localized proteoglycan secretion is less defined for construct regions stimulated by low fluid shears, as revealed by denser protein accumulation within the deeper sections of the scaffold. Note the small circular stained cluster located deep in the construct region for this hydrodynamic regime is likely a collection of nonviable cells settled to the bottom during cell-laden scaffold preparation. Regardless, this comparison of surface and deep tissue regions exposed to gradated surface fluid shears coincides with our argument assessing the fluid shear magnitude in which AC protein localization at the construct surface is regulated by the level of viscous surface shear.

IHC Staining. Our bioreactor culture findings demonstrate that our perfusion bioreactor system serves to differentiate MSCs to express chondrogenic genes, which contribute to their development of a dense ECM network more representative of AC production. With the goal of uncovering detailed ECM protein composition, we implemented IHC staining methods to further validate the cell chondrogenic commitment within a perfused environment. Similar to mRNA findings, fluorescent stained images for Sox9 in Figure 6A show abundant protein expression throughout the different layers of our cell construct that is considerably higher than static control samples. Earlier, we demonstrated that Sox9 gene upregulation corresponds to the expression of supporting chondrogenic genes. IHC protein stains of lubricin and COL2A1 in Figure 6B and ACAN and VCAN in Figure 6C collectively support this claim, in which Sox9-expressing cells within a perfused environment are secreting higher amounts of chondrogenic proteins. By comparison, static cell culture results reveal that chondrogenic differentiation is not well-established, as shown by the lesser abundance of AC protein markers. Rather, it is fibrocartilage collagen type I and hypertrophic collagen type X proteins that are primarily associated with this unstimulated sample. Though staining intensities for these proteins in addition to Runx2 are not as strong as we would expect from gene expression data, our characterizations of chondrogenic proteins for our control indicate less lubricin, type II collagen, and ACAN expression. Once again, we see that our bioreactor culture promotes cell chondrogenic commitment, which is further supported by protein expression of lubricin, COL2A1, and ACAN. Furthermore, our tracking of versican (VCAN), a proteoglycan present during MSC condensation and playing a pivotal role in cell chondrogenesis, also provides indication for cell differentiation. The IHC staining results show more abundant protein markers for COL1A1 and VCAN in cells stimulated by a high surface fluid shear regime. This is in contrast to MSCs grown within lower hydrodynamic shear environments in which there is a shift in protein markers in favor of moreabundant lubricin, COL2A1, and ACAN presence for medium fluid shears and COL2A1 and COL10A1 for low fluid shears. Here, our IHC findings, in addition to corroborating mRNA and histology data, support that a gradated fluid environment influences cell chondrogenic fate in which protein expression differs region by region.

DISCUSSION

To better discuss the overall trends in light of collective chondrogenic indicators, we summarize results in Table 1 for bioreactor chondro-inducing capabilities and contrast these results with findings in the literature. Arrows designated as green up, ▲, refer to increases in preferable qualities, and green down, ▼, to decreases in nonpreferred qualities. The red arrows, ▲ or ▼, respectively indicate undesirable increases or undesirable decreases in chondrogenic qualities. One overall trend in the key cell culture findings within Table 1 is the highly upregulated biomarkers, including Sox9, lubricin, ACAN, and type II collagen, confirming cell chondrogenesis for perfused constructs. In contrast, we see dramatically increased Runx2, COL1A1, and COL10A1 gene expressions along with less organized matrix synthesis for static controls, demonstrating undesirable cell movement from AC characteristics. We acknowledge that the data presented in these studies were obtained from cells sourced from a single donor. Given that MSC chondrogenesis varies across donors due to in vivo functional differences[34] and age- and gender-related conditions,[35] it will be important for future investigations to evaluate how cells from multiple donors respond to fluid flow and assess potential variability. Overall, our gradated fluid perfusion environment demonstrates improved chondrogenic differentiation. Next, we will discuss specific regions of our final 14 day construct and compare results to desirable qualities as they relate to trilayered AC development.

Our second objective is to understand whether varying magnitudes of fluid shear for the same cell construct led to regional differentiation of MSCs with cells expressing different types and amounts of chondrogenic markers, and if this protocol yields an anisotropic tissue moving tissue toward a striated construct similar to that of AC. Indeed, such differences exist for our engineered tissue. In Table 1, we see near the surface for high fluid shears improved chondrogenic gene upregulations for lubricin and COL2A1 by 33- and 5.4-fold, respectively. While the COL1A1 gene is also down-regulated here by 0.22-fold for both the surface and deep regions compared to the static control, cells within this hydrodynamic shear regime express nearly 2-fold higher COL1A1 levels compared to cells exposed to lower fluid shears. This is corroborated by our tabulated IHC characterizations showing adequate presence of lubricin, ACAN, and type II collagen, which further supports the formation of a surface-localized proteoglycan matrix. In addition, IHC findings at our highest shears reveal strong COL1A1 and VCAN expression, which is substantially higher than that found in any other tissue region. We see agreement with previously reported findings indicating production of a dense proteoglycan matrix supported by Safranin O staining with shear moduli enhancements by 66% for cell constructs stimulated by a high fluid shear regime in the 50−210 mPa range.[16,18] Specifically, Chen et al. report manufacturing of a superficial zone for a 14 day agarose-encapsulated chondrocyte

https://doi.org/10.1021/acsbiomaterials.5c01183
ACS Biomater. Sci. Eng. XXXX, XXX, XXX−XXX

study, where fluid shear stimulations of 120 mPa led to increased GAG production by 1.4-fold and considerable localization of COL2A1, ACAN, and lubricin proteins.[7] This is consistent with our observations for high surface shears, where gene upregulations and IHC stains demonstrate improved expression of similar differentiation markers. We conclude that our surface fluid shear in the 22−41 mPa range contributes to the differentiation of MSCs to an ACh lineage moving toward superficial zone-like ECM properties, as supported by strong lubricin gene expression and adequate protein production of type II collagen molecules.

Next, we track the change in MSC maturation as the surface hydrodynamic environment transitions to medium fluid shears in the 4.5−8.4 mPa range, where we see both superficial and middle zone chondrogenic properties. As shown in Table 1, we observe a maximum upregulation of ACAN and lubricin genes by 2.1 and 40-fold, respectively, that is considerably higher than neighboring regions, in addition to correspondingly high levels of Sox9 and COL2A1 genes by 1.8 and 5.8-fold, respectively, compared to that of static control tissue. Further support comes from Safranin O staining, where we detect concentrated proteoglycan synthesis at the tissue surface, and IHC staining for ACAN being the strongest of any region and Sox9, lubricin, and COL2A1 proteins being among the strongest in comparison to other regions. Similar findings are present in the literature for viscous shear in the 4.6−6.7 mPa range, where perfusion bioreactor studies result in a 100% increase for COL2A1/COL1A1 Western blot protein density and a 4.5% increase for GAG deposition compared to static control samples.[8,33] Work completed by Raimondi et al.[8] provides insights about recapitulating a gradated interstitial fluid shear environment for chondrocytes seeded onto a porous polyurethane foam where they experiment with hydrodynamic interstitial shears in the 4.6−56 mPa range. At 4.6 mPa, their results indicate a maximum increase of GAG content 28% higher than cells stimulated by the higher 56 mPa shear level. Though our biochemical characterizations show minor variation between fluid shear groups, we do see a similar trend for our mRNA, histology, and IHC analyses, where sGAG and collagen expression, particularly ACAN and COL2A1, are improved for our manufactured cell construct at the medium shear range. The high levels of ACAN, COL2A1, and lubricin at this shear range resemble chondrogenic markers for superficial zone lubrication as well as middle zone increases in ACAN presence.[20,36]

In our assessment of the MSC fate for low surface fluid shear in the 2.2−3.8 mPa range, we observe changes in differentiation markers somewhat more representative of hypertrophic behavior. Cell mRNA expressions in Table 1 support this, where Sox9 is downregulated by 0.96-fold compared to upregulations of 1.5 and 1.8-fold in the respective high and medium surface shear ranges. Most notably, cell characterizations for this construct region indicate improved likelihood of collagen formation with an 8.0-fold increase in COL2A1 and a maximum value of 0.01-fold for COL10A1, the latter being 2.5-fold above the high shear region and 1.4-fold above the medium shear region, which is validated qualitatively by IHC protein stains. Corroborative evidence from literature shows a 155% increase in total collagen secretion and 108-fold higher COL2A1 expression for very low shear regions resulting from fluid velocities in the 1 to 10 μm/s range when compared to static conditions.[13,31] Of further support is work by Raimondi et al.[33] where western blot protein density for ACh-seeded polyurethane foams shows maximum COL2A1/COL1A1 levels for fluid shears of 1 mPa. In their observation, they correlate COL2A1/COL1A1 increases to fluid shear magnitude, in which 1 mPa hydrodynamic shears promoted COL2A1 protein synthesis with considerably less hypertrophic COL1A1 protein expression. This ratio was 286% higher than static controls and 109% higher than a 7 mPa fluid shear magnitude. Our findings also show statistically lower values for COL1A1 gene expression with 0.59- and 0.87-fold reductions compared to the respective high and medium shear ranges, favoring COL2A1 protein expression over COL1A1 as shown further by IHC stains. Assessing the data collectively, we show our lowest surface shears move cells toward a slightly more hypertrophic fate, expressing more COL10A1 mRNA and corresponding protein levels, resembling more what is expected of cells located in deep zone AC that produce a mineralized matrix higher in type X collagen.[24] The transition in this zonal region provides supporting evidence that MSCs are moving toward a mature ACh lineage with characteristics similar to the deep zone near the subchondral bone, where hypotrophy is known to occur.[26]

Finally, looking at deep tissue properties for our cell construct shown in the first column of Table 1, less desirable characteristics infer that some level of direct stimulation, in our case fluid perfusion, is more important than the position within the tissue. Specifically for the deep or subsurface regions, ACAN across all shear levels falls to the 0.59−0.93-fold range with respect to the static control. COL2A1 is significantly lower in all cases than that of the surface, and Sox9 is in the 0.65−0.96-fold range for the deep region for the high and medium shears. In the low shear range, gene expressions for Sox9 and lubricin are high; however, as stated, other chondrogenic indices are in a less desirable range. These data strongly infer that some form of mechanical stimulation is required for subsurface cell regions to achieve similar proteoglycan levels exhibited by the AC Deep zone found in vivo, which provides compressive strength.[37,38] This is supported by previous work from our group in studying AChs in porous chitosan−agarose (CHAG) scaffolds and interstitial fluid shear of 40 mPa shows dramatic improvements compared to nonperfused samples in chondrogenic gene expression and matrix synthesis.[32] This lays the groundwork for further investigation of cell maturation in relation to vertical depth in combining porous scaffolds through which the medium will perfuse in our gradated fluid shear environment.

CONCLUSIONS AND FUTURE DIRECTIONS

In summary, our work demonstrates that providing a broad hydrodynamic regime, in our case fluid perfusion within a bioreactor, regulates the MSC chondrogenic fate. Beginning with our COMSOL simulation, our modeling for our tapered perfusion bioreactor shows that fluid velocities and surface shears will result in a gradation in magnitude for each parallel cell chamber due to the changing cross-sectional area of the cell chamber design. By implementing a range of cell culture characterizations, we show differences in cell expression related to the heterogeneous hydrodynamic environment and relate our findings to what is known about chondrogenic markers associated with superficial, middle, and deep zone AC. Most notably, our work along, with supporting literature evidence, lays the groundwork for designing systems capable of generating a trilayered cartilage construct. Limitations in the work include a need for better staining of the proteins within

https://doi.org/10.1021/acsbiomaterials.5c01183
ACS Biomater. Sci. Eng. XXXX, XXX, XXX−XXX

the matrix rather than those within and around the cells. For this, an improved method for IHC should be used to reveal extracellular matrix proteins, not just those within the cell, as this has been done in numerous other studies.[7,15] Future studies are also needed in a reformed multichamber system to maintain a more uniform fluid flow gradient between all nine parallel subunit bioreactors by increasing the depth of the inlet manifold to create a much smaller pressure drop through the manifold to decrease variation from one bioreactor well to another. Throughout our work, we primarily discuss the effects of fluid shear stress, as it contributes to chondrogenic cell differentiation. While this aspect is critical for understanding how cells respond to mechanical signaling, additional factors such as nutrient transportation by fluid flow also demonstrate improvements for cell growth and differentiation that may be at play.[39,40] Further understanding of nutrient transport issues is needed for studies using a unique fluid perfusion environment similar to the one addressed in our work. In addition, in vivo hydrostatic pressure is known to be a contributing mechanical factor in the native AC environment. For example, previous researchers have shown cells exposed to oscillating hydrostatic pressure (OHP) magnitudes ranging from 0.1 to 10 MPa have strongly increased Sox9 mRNA expression by 4-fold, which leads to abundant gene upregulation and protein expression of chondrogenic markers supporting enhanced tissue biomechanics.[41−45] Future considerations include combining surface fluid shear gradients, porous supports, and OHP, where their additive effects are expected to lead to production of a more distinct trilayered tissue with stronger regional characteristics similar to zonal AC organization. MSCs pooled from multiple donors also expand the generalizability of such studies.

■ ASSOCIATED CONTENT

Supporting Information

The Supporting Information is available free of charge at https://pubs.acs.org/doi/10.1021/acsbiomaterials.5c01183.

List of genes of interest provided with primer information; details of sources and specificity of antihuman antibodies; microtome orientation for bioreactor samples supporting histology and IHC stains; live/dead images indicating cell viability; and dye videography of perfusion bioreactor confirming COMSOL modeling (PDF)

■ AUTHOR INFORMATION

Corresponding Author

Bernard J. Van Wie − *Voiland School of Chemical Engineering and Bioengineering, Washington State University, Pullman, Washington 99164, United States;* orcid.org/0000-0001-7382-9715; Phone: (509) 335-4103; Email: bvanwie@wsu.edu

Authors

Terreill J. Robertson, II − *Voiland School of Chemical Engineering and Bioengineering, Washington State University, Pullman, Washington 99164, United States*

Alec W. Schuler − *School of Mechanical and Materials Engineering, Washington State University, Pullman, Washington 99164, United States*

Pakkanpat P. Pondipornnont − *Voiland School of Chemical Engineering and Bioengineering, Washington State University, Pullman, Washington 99164, United States*

Ryan R. Driskell − *School of Molecular Biosciences, Washington State University, Pullman, Washington 99164, United States*

Lawrence J. Bonassar − *Meinig School of Biomedical Engineering, Cornell University, Ithaca, New York 14850, United States;* orcid.org/0000-0003-1094-6433

Arda Gozen − *School of Mechanical and Materials Engineering, Washington State University, Pullman, Washington 99164, United States*

Wenji Dong − *Voiland School of Chemical Engineering and Bioengineering, Washington State University, Pullman, Washington 99164, United States*

David B. Thiessen − *Voiland School of Chemical Engineering and Bioengineering, Washington State University, Pullman, Washington 99164, United States*

Complete contact information is available at: https://pubs.acs.org/10.1021/acsbiomaterials.5c01183

Notes

The authors declare no competing financial interest.

■ ACKNOWLEDGMENTS

This work was supported by NSF CBET Nos. 2225528, 2225559, and GOALI 1606226. We thank Eric Barrow, Evelyn Aguilar, and Miles Pepper for manufacturing the TBR system. We also would like to thank Peter Pusateri, an undergraduate research assistant, for his assistance with histological staining of cell constructs. We also are grateful for staff at the Franceschi Microscopy and Imaging Center located on Washington State University Pullman campus for training in the use of their confocal microscope used to produce images in this work. Finally, we would like to acknowledge the use of the BioRender platform for creating figures supporting this work.

■ REFERENCES

(1) Makris, E. A.; Gomoll, A. H.; Malizos, K. N.; Hu, J. C.; Athanasiou, K. A. Repair and Tissue Engineering Techniques for Articular Cartilage. *Nat. Rev. Rheumatol.* **2015**, *11* (1), 21−34.

(2) Darling, E. M.; Athanasiou, K. A. Rapid Phenotypic Changes in Passaged Articular Chondrocyte Subpopulations. *J. Orthop. Res.* **2005**, *23* (2), 425−432.

(3) Bullough, P.; Goodfellow, J. The significance of the fine structure of articular cartilage. *J. Bone Jt. Surg.* **1968**, *50* (4), 852−857.

(4) Panadero, J. A.; Lanceros-Mendez, S.; Ribelles, J. L. G. Differentiation of Mesenchymal Stem Cells for Cartilage Tissue Engineering: Individual and Synergetic Effects of Three-Dimensional Environment and Mechanical Loading. *Acta Biomater.* **2016**, *33*, 1−12.

(5) Grassel, S.; Ahmed, N. Influence of Cellular Microenvironment and Paracrine Signals on Chondrogenic Differentiation. *Front. Biosci. J. Virtual Library* **2007**, *12*, 4946−4956.

(6) Responte, D. J.; Lee, J. K.; Hu, J. C.; Athanasiou, K. A. Biomechanics-driven Chondrogenesis: From Embryo to Adult. *FASEB J.* **2012**, *26* (9), 3614−3624.

(7) Chen, T.; Hilton, M. J.; Brown, E. B.; Zuscik, M. J.; Awad, H. A. Engineering Superficial Zone Features in Tissue Engineered Cartilage. *Biotechnol. Bioeng.* **2013**, *110* (5), 1476−1486.

(8) Raimondi, M. T.; Moretti, M.; Cioffi, M.; Giordano, C.; Boschetti, F.; Laganà, K.; Pietrabissa, R. The Effect of Hydrodynamic Shear on 3D Engineered Chondrocyte Systems Subject to Direct Perfusion. *Biorheology* **2006**, *43* (3−4), 215−222.

(9) Guo, T.; Yu, L.; Lim, C. G.; Goodley, A. S.; Xiao, X.; Placone, J. K.; Ferlin, K. M.; Nguyen, B.-N. B.; Hsieh, A. H.; Fisher, J. P. Effect of Dynamic Culture and Periodic Compression on Human Mesenchymal Stem Cell Proliferation and Chondrogenesis. *Ann. Biomed. Eng.* **2016**, *44* (7), 2103−2113.
(10) Salinas, E. Y.; Hu, J. C.; Athanasiou, K. A Guide for Using Mechanical Stimulation to Enhance Tissue-Engineered Articular Cartilage Properties. *Tissue Eng., Part B* **2018**, *24* (5), 345−358.
(11) Vunjak-Novakovic, G.; Martin, I.; Obradovic, B.; Treppo, S.; Grodzinsky, A. J.; Langer, R.; Freed, L. E. Bioreactor Cultivation Conditions Modulate the Composition and Mechanical Properties of Tissue-engineered Cartilage. *J. Orthop. Res.* **1999**, *17* (1), 130−138.
(12) Sharifi, N.; Gharravi, A. M. Shear Bioreactors Stimulating Chondrocyte Regeneration, a Systematic Review. *Inflammation Regener.* **2019**, *39* (1), 16.
(13) Pazzano, D.; Mercier, K. A.; Moran, J. M.; Fong, S. S.; DiBiasio, D. D.; Rulfs, J. X.; Kohles, S. S.; Bonassar, L. J. Comparison of Chondrogensis in Static and Perfused Bioreactor Culture. *Biotechnol. Prog.* **2000**, *16* (5), 893−896.
(14) Xu, X.; Urban, J. P. G.; Tirlapur, U.; Wu, M.; Cui, Z.; Cui, Z. Influence of Perfusion on Metabolism and Matrix Production by Bovine Articular Chondrocytes in Hydrogel Scaffolds. *Biotechnol. Bioeng.* **2006**, *93* (6), 1103−1111.
(15) Forsey, R. W.; Tare, R.; Oreffo, R. O. C.; Chaudhuri, J. B. Perfusion Bioreactor Studies of Chondrocyte Growth in Alginate-Chitosan Capsules. *Biotechnol. Appl. Biochem.* **2012**, *59* (2), 142−152.
(16) Gemmiti, C. V.; Guldberg, R. E. Shear Stress Magnitude and Duration Modulates Matrix Composition and Tensile Mechanical Properties in Engineered Cartilaginous Tissue. *Biotechnol. Bioeng.* **2009**, *104* (4), 809−820.
(17) Gemmiti, C. V.; Guldberg, R. E. Fluid Flow Increases Type II Collagen Deposition and Tensile Mechanical Properties in Bioreactor-Grown Tissue-Engineered Cartilage. *Tissue Eng.* **2006**, *12* (3), 469−479.
(18) Salinas, E. Y.; Aryaei, A.; Paschos, N.; Berson, E.; Kwon, H.; Hu, J. C.; Athanasiou, K. A. Shear Stress Induced by Fluid Flow Produces Improvements in Tissue-Engineered Cartilage. *Biofabrication* **2020**, *12* (4), 045010.
(19) Lefebvre, V.; Smits, P. Transcriptional Control of Chondrocyte Fate and Differentiation. *Birth Defects Res., Part C* **2005**, *75* (3), 200−212.
(20) Behonick, D. J.; Werb, Z. A Bit of Give and Take: The Relationship between the Extracellular Matrix and the Developing Chondrocyte. *Mech. Dev.* **2003**, *120* (11), 1327−1336.
(21) Kannan, S.; Gokul Krishna, S.; Gupta, P. K.; Kolkundkar, U. K. Advantages of Pooling of Human Bone Marrow-Derived Mesenchymal Stromal Cells from Different Donors versus Single-Donor MSCs. *Sci. Rep.* **2024**, *14* (1), 12654.
(22) Siegel, G.; Kluba, T.; Hermanutz-Klein, U.; Bieback, K.; Northoff, H.; Schäfer, R. Phenotype, Donor Age and Gender Affect Function of Human Bone Marrow-Derived Mesenchymal Stromal Cells. *BMC Med.* **2013**, *11* (1), 146.
(23) Scibetta, A. C.; Morris, E. R.; Liebowitz, A. B.; Gao, X.; Lu, A.; Philippon, M. J.; Huard, J. Characterization of the Chondrogenic and Osteogenic Potential of Male and Female Human Muscle-derived Stem Cells: Implication for Stem Cell Therapy. *J. Orthop. Res.* **2019**, *37* (6), 1339−1349.
(24) Maxwell, C. J.; Soltisz, A. M.; Rich, W. W.; Choi, A.; Reilly, M. A.; Swindle-Reilly, K. E. Tunable Alginate Hydrogels as Injectable Drug Delivery Vehicles for Optic Neuropathy. *J. Biomed. Mater. Res., Part A* **2022**, *110* (10), 1621−1635.
(25) Freeman, F. E.; Kelly, D. J. Tuning Alginate Bioink Stiffness and Composition for Controlled Growth Factor Delivery and to Spatially Direct MSC Fate within Bioprinted Tissues. *Sci. Rep.* **2017**, *7* (1), 17042.
(26) Xie, L.; Zhang, N.; Marsano, A.; Vunjak-Novakovic, G.; Zhang, Y.; Lopez, M. J. In Vitro Mesenchymal Trilineage Differentiation and Extracellular Matrix Production by Adipose and Bone Marrow Derived Adult Equine Multipotent Stromal Cells on a Collagen Scaffold. *Stem Cell Rev. Rep.* **2013**, *9* (6), 858−872.
(27) Tığlı, R. S.; Cannizaro, C.; Gümüşderelioğlu, M.; Kaplan, D. L. Chondrogenesis in Perfusion Bioreactors Using Porous Silk Scaffolds and hESC-derived MSCs. *J. Biomed. Mater. Res., Part A* **2011**, *96* (1), 21−28.
(28) Amr, M.; Mallah, A.; Yasmeen, S.; Van Wie, B.; Gozen, A.; Mendenhall, J.; Abu-Lail, N. I. From Chondrocytes to Chondrons, Maintenance of Phenotype and Matrix Production in a Composite 3D Hydrogel Scaffold. *Gels* **2022**, *8* (2), 90.
(29) Van Wie, B. J. Enhancing Adipose Stem Cell Chondrogenesis: A Study on the Roles of Dexamethasone, Transforming Growth Factor B3 and Ascorbate Supplements and Their Combination. *J. Stem Cell Ther. Transplant.* **2017**, *1* (1), 028−051.
(30) Lefebvre, V.; Dvir-Ginzberg, M. SOX9 and the Many Facets of Its Regulation in the Chondrocyte Lineage. *Connect. Tissue Res.* **2017**, *58* (1), 2−14.
(31) Silva, J. C.; Moura, C. S.; Borrecho, G.; de Matos, A. P. A.; da Silva, C. L.; Cabral, J. M. S.; Bártolo, P. J.; Linhardt, R. J.; Ferreira, F. C. Extruded Bioreactor Perfusion Culture Supports the Chondrogenic Differentiation of Human Mesenchymal Stem/Stromal Cells in 3D Porous Poly(ε-Caprolactone) Scaffolds. *Biotechnol. J.* **2020**, *15* (2), No. e1900078.
(32) Abusharkh, H. A.; Robertson, T.; Mendenhall, J.; Gozen, B. A.; Tingstad, E. M.; Abu-Lail, N. I.; Thiessen, D. B.; Van Wie, B. J. Impact of Interstitial Flow on Cartilage Matrix Synthesis and NF-kB Transcription Factor mRNA Expression in a Novel Perfusion Bioreactor. *Biotechnol. Prog.* **2024**, *40* (1), No. e3404.
(33) Raimondi, M. T.; Candiani, G.; Cabras, M.; Cioffi, M.; Laganà, K.; Moretti, M.; Pietrabissa, R. Engineered Cartilage Constructs Subject to Very Low Regimens of Interstitial Perfusion. *Biorheology* **2008**, *45* (3−4), 471−478.
(34) Rothweiler, R.; Basoli, V.; Duttenhoefer, F.; Kubosch, D.; Schmelzeisen, R.; Johnstone, B.; Alini, M.; Stoddart, M. J. Predicting and Promoting Human Bone Marrow MSC Chondrogenesis by Way of TGFβ Receptor Profiles: Toward Personalized Medicine. *Front. Bioeng. Biotechnol.* **2020**, *8*, 618.
(35) Kim, M.; Erickson, I. E.; Huang, A. H.; Garrity, S. T.; Mauck, R. L.; Steinberg, D. R. Donor Variation and Optimization of Human Mesenchymal Stem Cell Chondrogenesis in Hyaluronic Acid. *Tissue Eng., Part A* **2018**, *24* (21−22), 1693−1703.
(36) Camarero-Espinosa, S.; Rothen-Rutishauser, B.; Foster, E. J.; Weder, C. Articular Cartilage: From Formation to Tissue Engineering. *Biomater. Sci.* **2016**, *4* (5), 734−767.
(37) Sophia Fox, A. J.; Bedi, A.; Rodeo, S. A. The Basic Science of Articular Cartilage: Structure, Composition, and Function. *Sports Health* **2009**, *1* (6), 461−468.
(38) Buckwalter, J. A.; Mankin, H. J.; Grodzinsky, A. J. Articular Cartilage and Osteoarthritis. *Instr. Course Lect.* **2005**, *54*, 465−480.
(39) DiDomenico, C. D.; Xiang Wang, Z.; Bonassar, L. J. Cyclic Mechanical Loading Enhances Transport of Antibodies Into Articular Cartilage. *J. Biomech. Eng.* **2017**, *139* (1), 011012.
(40) Bonassar, L. J.; Grodzinsky, A. J.; Frank, E. H.; Davila, S. G.; Bhaktav, N. R.; Trippel, S. B. The Effect of Dynamic Compression on the Response of Articular Cartilage to Insulin-like Growth factor-I. *J. Orthop. Res.* **2001**, *19* (1), 11−17.
(41) Angele, P.; Yoo, J. U.; Smith, C.; Mansour, J.; Jepsen, K. J.; Nerlich, M.; Johnstone, B. Cyclic Hydrostatic Pressure Enhances the Chondrogenic Phenotype of Human Mesenchymal Progenitor Cells Differentiated in Vitro. *J. Orthop. Res.* **2003**, *21* (3), 451−457.
(42) Aprile, P.; Kelly, D. J. Hydrostatic Pressure Regulates the Volume, Aggregation and Chondrogenic Differentiation of Bone Marrow Derived Stromal Cells. *Front. Bioeng. Biotechnol.* **2021**, *8*, 619914.
(43) Miyanishi, K.; Trindade, M. C. D.; Lindsey, D. P.; Beaupré, G. S.; Carter, D. R.; Goodman, S. B.; Schurman, D. J.; Smith, R. L. Effects of Hydrostatic Pressure and Transforming Growth Factor-β 3 on Adult Human Mesenchymal Stem Cell Chondrogenesis *In Vitro*. *Tissue Eng.* **2006**, *12* (6), 1419−1428.

https://doi.org/10.1021/acsbiomaterials.5c01183
ACS Biomater. Sci. Eng. XXXX, XXX, XXX−XXX

(44) Elder, B. D.; Athanasiou, K. A. Synergistic and Additive Effects of Hydrostatic Pressure and Growth Factors on Tissue Formation. *PLoS One* **2008**, *3* (6), No. e2341.
(45) Nazempour, A.; Quisenberry, C. R.; Abu-Lail, N. I.; Van Wie, B. J. Combined Effects of Oscillating Hydrostatic Pressure, Perfusion and Encapsulation in a Novel Bioreactor for Enhancing Extracellular Matrix Synthesis by Bovine Chondrocytes. *Cell Tissue Res.* **2017**, *370* (1), 179−193.

https://doi.org/10.1021/acsbiomaterials.5c01183
ACS Biomater. Sci. Eng. XXXX, XXX, XXX−XXX